

Approaching ultimate SNR and ideal current patterns with finite surface coil arrays on a dielectric cylinder

R. Lattanzi^{1,2}, A. K. Grant^{2,3}, and D. K. Sodickson⁴

¹Division of Health Sciences and Technology, Harvard-MIT, Cambridge, MA, United States, ²Radiology, Beth Israel Deaconess Medical Center, Boston, MA, United States, ³Harvard Medical School, Boston, MA, United States, ⁴New York University Medical Center, New York, NY, United States

Introduction

In parallel imaging techniques, the number of elements in the receive coil array, as well as their geometrical arrangement, is fundamental for achieving many-fold accelerations. As the number of channels available in MR systems has increased to enable faster acquisitions, building prototypes of coil arrays has become more difficult and expensive, and therefore the design of coil arrays has relied ever more upon electrodynamic simulations. Calculations of the ultimate intrinsic signal-to-noise ratio (SNR) have indicated that there is an intrinsic limit to the acceleration capabilities of parallel imaging [1,2]. Recent work has shown that knowledge of this limit can be used as a reference to choose an acceptable number and size of coil elements during the design of a coil array [3], as well as to assess the absolute performance of existing arrays [4]. In this study we calculate the ultimate intrinsic SNR in the case of a dielectric cylinder and we investigate how rapidly the optimum can be reached with “cylindrical window” coil arrays, uniformly distributed around the surface of the object. We used a realistic noise model, in order to account for losses due to the coil conductors, to the receive circuit and to the conductive shield of the MR system. Ideal current patterns, resulting in the highest possible SNR, were compared with the current patterns associated with the finite arrays.

Theory and Methods

The sample was modeled as a dielectric cylinder, with a radius $\rho = 20$ cm and a length $L = 90$ cm, assuming dielectric properties of dog skeletal muscle. A complete set \mathbf{K} of current functions distributed on a cylindrical surface A , concentric with the cylindrical body and with radius 5 mm larger, was derived following a method outlined by Schnell et al. [5]. Each current mode in \mathbf{K} takes the form: $k_n(m) = W_n^{(1)}(m)\nabla \times e^{im\phi} e^{imz} \hat{\rho} + W_n^{(2)}(m)\nabla e^{im\phi} e^{imz}$. $W_n^{(1)}(m)$ and $W_n^{(2)}(m)$ are the series expansion

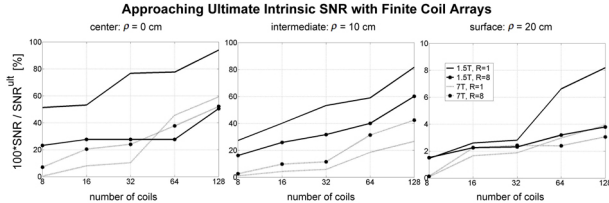


Fig. 1 SNR, normalized to the ultimate intrinsic SNR, as a function of number of coil elements, at various positions along the radius ρ of the dielectric cylinder, for different values of main magnetic field strength and acceleration factor.

coefficients, ρ , ϕ and z are the radial, azimuthal and axial coordinates, respectively. Ultimate intrinsic SNR at a generic voxel n was calculated for Cartesian SENSE reconstructions [6] as:

$SNR_n^{ult} \propto \omega_0 B_0 / \sqrt{4k_B T_s (\mathbf{X}\mathbf{R}^{-1}\mathbf{X}^H)_m^{-1}}$, where ω_0 is the Larmor frequency, B_0 is the main magnetic field strength, k_B is Boltzmann’s constant, T_s is the temperature of the sample and the superscript H indicates a conjugate transpose. The matrix $\mathbf{X}=\mathbf{I}\mathbf{S}$ is the mode sensitivity matrix \mathbf{S} , multiplied by a transformation matrix \mathbf{T} that accounts for boundary conditions at the surface of the object. The noise resistance \mathbf{R} was calculated as $\mathbf{R} = \mathbf{T}\mathbf{R}_L\mathbf{T}^H + \mathbf{R}_A + \mathbf{U}\mathbf{R}_S\mathbf{U}^H$, where

$$R_{L(i,j)} = \int_V \sigma(\mathbf{r}) e_j^*(\mathbf{r}, t) \cdot e_i(\mathbf{r}, t) d\mathbf{r}$$

(with σ being the sample conductivity and $e_i(\mathbf{r}, t)$ the electric field generated by a unit current on the i^{th} mode) accounts for sample losses,

$$R_{A(i,j)} = 1/(d_c \sigma_c) \int_A k_j^*(\mathbf{r}, t) \cdot k_i(\mathbf{r}, t) \rho dA$$

(with σ_c being the conductivity of the coil material, d_c its thickness and $k_i(\mathbf{r}, t)$ the current distribution of the i^{th} mode) accounts for losses in the conductors and

$$R_{S(i,j)} = 1/(d_s \sigma_s) \int_A k_{s,j}^*(\mathbf{r}, t) \cdot k_{s,i}(\mathbf{r}, t) \rho_s dA$$

(with σ_s being the conductivity of the shield, d_s its thickness, ρ_s its distance from the center of the cylinder and $k_{s,j}(\mathbf{r}, t)$ the current distribution induced on the shield by the magnetic field of the i^{th} mode) accounts for losses in the conductive shield. The transformation matrix \mathbf{U} sets the boundary conditions at the shield surface, which was positioned at $\rho_s = 34.25$ cm. The current density distribution on the shield, which was not included in Schnell’s model [5], can be calculated with the same dyadic Green’s function formulation [7]: $\mathbf{K}_s(\mathbf{r}, t) = 1/\mu_0 \mathbf{B}(\mathbf{r}, t)|_{\rho=\rho_s} \times \hat{\rho}$, where \mathbf{B} is a matrix containing the value of the modes’ magnetic field for $\rho = \rho_s$. Ideal surface current

patterns were computed by multiplying the modes’ current distributions $k_n(m)$ with the SNR-optimal weights from the SENSE reconstruction [5,6] and summing. The SNR and the current patterns for the case of finite cylindrical window coil arrays were calculated using the same computational framework, expressing the current distributions of each coil by means of current delta functions. The SNR for the finite coil arrays was multiplied by an additional noise term, describing for each channel the noise loss of the entire receive chain (noise figure = 1.1 dB). Different array configurations were generated by arranging identical coil elements around the cylinder and along its axial direction. For both coils and shield we assumed copper conductivity and conductor thickness equal to skin depth. Calculations were repeated for different values of the main magnetic field strength and various acceleration factors.

Results and Discussion

Figure 1 shows the convergence of SNR toward the ultimate value, as a function of number of coil elements in the array, for a reconstructed pixel in the center of cylinder (leftmost plot), halfway along its radius (central plot) and at its surface (rightmost plot). 1.5T (solid line) and 7T (dotted line) magnetic field strengths were considered, for R=1 (line only) and R=8 (line with solid circles) accelerations in the L-R direction. The number of coils distributed around the circumference of the cylinder was always at least twice the number of coils along the axial direction (e.g. 32-element array = 8 coils arranged circumferentially repeated 4 times along the axis). In the center, ultimate SNR can nearly be reached with 128 elements, whereas near the surface ultimate SNR grows exponentially and the gap is an order of magnitude larger. At higher magnetic field strength, the accelerated behavior with respect to the optimum for some cases is better than the unaccelerated (i.e. accelerated SNR approaches more closely the ultimate accelerated SNR than the unaccelerated SNR approaches its ultimate value). Figure 2 compares ideal surface current patterns with the weighted current patterns for two array configurations, for a reconstructed pixel in the center of the cylinder, in the unaccelerated case at 7T. As expected from the convergence plots in figure 1, current patterns that results in ultimate SNR are approximated better with 128 coils than with 8 coils. The complex distribution of the ideal current patterns shows superposition of closed-loop type currents with electric dipole behavior, suggesting that the “cylindrical window” geometry may not be the best choice at ultrahigh field strengths.

Conclusions

In this work we have extended a previously published method [5] for calculating ultimate intrinsic SNR in the case of a dielectric cylinder. We have adapted the theoretical framework for parallel imaging reconstructions and we have included the MR conductive shield in the model. The ultimate SNR behavior was compared with the case of finite coil arrays. Near the center of the object, at low magnetic field strengths, more than 50% of the optimum can be achieved with small arrays. Near the edge, ultimate SNR is not approached even with very large arrays, with our particular choice of coil geometry. Ideal surface current patterns can be used as a reference to find improved coil array designs.

References

- [1] Ohliger MA et al (2003), MRM 50: 1018-1030 [2] Wiesinger F et al (2004), MRM 52:953-964 [3] Wiesinger F et al, ISMRM 2005, 672
 [4] Lattanzi R et al, ISMRM 2006, 424 [5] Schnell W et al, (2000), IEEE Trans Ant Prop 48:418-28 [6] Pruessman KP et al (1999), MRM 42:952-962.
 [7] Tai CT, Dyadic Green Functions in Electromagnetic Theory (1994)

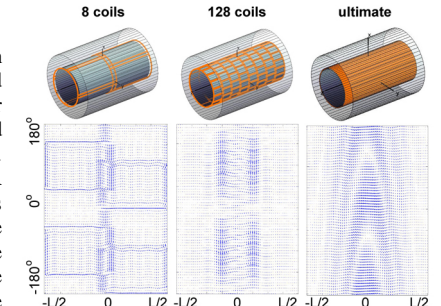


Fig. 2 Ideal surface current patterns compared with surface current patterns from cylindrical window coil arrays, for a reconstructed pixel in the center of the object, in the unaccelerated case at 7T. The plots represent 2D “unwrapped” views of the 3D cylindrical surface. The axial and the azimuthal coordinates are on the horizontal and the vertical axis, respectively.